Critical Behavior of Three-Dimensional Disordered Potts Models with Many States

R. Alvarez Baños,[1,2] A. Cruz,[1,2] L. A. Fernandez,[3,2] A. Gordillo-Guerrero,[4,2] J. M. Gil-Narvion,[1,2] M. Guidetti,[5] A. Maiorano,[6] F. Mantovani,[5] E. Marinari,[6] V. Martin-Mayor,[3,2] J. Monforte-Garcia,[1,2] A. Muñoz Sudupe,[3] D. Navarro,[7] G. Parisi,[6] S. Perez-Gaviro,[6,2] J. J. Ruiz-Lorenzo,[8,2] B. Seoane,[3,2] S. F. Schifano,[9] A. Tarancon,[1,2] R. Tripiccione,[5] and D. Yllanes[3,2]

[1]*Departamento de Física Teórica, Universidad de Zaragoza, 50009 Zaragoza, Spain.*
[2]*Instituto de Biocomputación y Física de Sistemas Complejos (BIFI), Zaragoza, Spain.*
[3]*Departamento de Física Teórica I, Universidad Complutense, 28040 Madrid, Spain.*
[4]*Dpto. de Ingeniería Eléctrica, Electrónica y Automática, Universidad de Extremadura, 10071 Cáceres, Spain.*
[5]*Dipartimento di Fisica, Università di Ferrara and INFN - Sezione di Ferrara, Ferrara, Italy.*
[6]*Dipartimento di Fisica, CNR and INFN, Università di Roma "La Sapienza", 00185 Roma, Italy.*
[7]*Departamento de Ingeniería, Electrónica y Comunicaciones and Instituto de Investigación en Ingeniería de Aragón (I3A), Universidad de Zaragoza, 50018 Zaragoza, Spain.*
[8]*Departamento de Física, Universidad de Extremadura, 06071 Badajoz, Spain.*
[9]*Dipartimento di Matematica, Università di Ferrara and INFN - Sezione di Ferrara, Ferrara, Italy.*

(Dated: May 6, 2010)

We study the $3D$ Disordered Potts Model with $p = 5$ and $p = 6$. Our numerical simulations (that severely slow down for increasing p) detect a very clear spin glass phase transition. We evaluate the critical exponents and the critical value of the temperature, and we use known results at lower p values to discuss how they evolve for increasing p. We do not find any sign of the presence of a transition to a ferromagnetic regime.

PACS numbers: 75.50.Lk, 75.40.Mg, 64.60.F-

I. INTRODUCTION

The three dimensional ($3D$) disordered Potts model (DPM) is an important system, that could help in clarifying a number of open and crucial questions. The first issue that comes to the mind is the possibility of understanding the glass transition, since this is a very challenging problem. On more general grounds, it is very interesting to try and qualify the behavior of the system when the number of states p becomes large: here we should see the paradigm of a "hard", first order like transition but, as we will discuss in the following, only sometimes this turns out to be clear (see for example the set of large scale, very accurate numerical simulations of Ref. 1, dealing with a model slightly different from the one defined here).

In such a difficult situation extensive numerical simulations are more than welcome, and the Janus supercomputer[2,3], optimized for studying spin glasses, reaches its peak performances when analyzing lattice regular systems based on variables that can take a finite, small number of values: disordered Potts models fit very well these requirements. Using the computational power of Janus we have been able to consistently thermalize the DPM with $p = 5$ and 6 on $3D$ (simple cubic) lattice systems with periodic boundary conditions and size up to $L = 12$. Bringing these systems to thermal equilibrium becomes increasingly harder with increasing number of states: it has been impossible for us, even by using a large amount of time of Janus (that for these problems performs, as we discuss better in the following, as thousands of PC processors), to get a significant, unbiased number of samples thermalized, and reliable measurements of physical quantities, for $p \geq 5$ on a $L = 16$ lattice.

Our results lead us to the claim that the critical behavior of the DPM with a large number of states p is very subtle, and if p is larger than, say, 5, numerical simulations could easily give misleading hints. The numerical results that we will discuss in the following lead us to believe that the spin glass transition gets stronger with increasing number of states p: a theoretical analysis of these results suggests that the transition could eventually become of first order for p large enough. We do not observe, for both $p = 5$ and $p = 6$, any sign of the presence of a spontaneous magnetization.

II. MODEL AND OBSERVABLES

We have performed numerical simulations of the DPM on a simple cubic lattice of linear size L with periodic boundary conditions. The Hamiltonian of the DPM is

$$\mathcal{H} \equiv -\sum_{\langle i,j \rangle} J_{ij}\, \delta_{s_i,s_j}\,, \tag{1}$$

where the sum is taken over all pairs of first neighboring sites. In the p-states model spins s_i can take p different values $\{0, 1, \ldots, p-1\}$. In this work we analyze the $p = 5$ and 6 cases. The couplings J_{ij} are independent random variables taken from a bimodal probability distribution ($J_{ij} = \pm 1$ with probability $\frac{1}{2}$). For a different definition of a disordered Potts model see Ref. 4.

It is convenient to rewrite the variables of the Potts model using the *simplex* representation, where the p Potts

states are described as vectors pointing to the corners of a $(p-1)$ dimensional hyper-tetrahedron. The Potts scalar spins s_i are thus written as $(p-1)$-dimensional unit vectors $\boldsymbol{S}_i$ satisfying the relations

$$\boldsymbol{S}_a \cdot \boldsymbol{S}_b = \frac{p\,\delta_{ab} - 1}{p-1}\,, \tag{2}$$

where a and $b \in [1,p]$. We use this vector representation to define the observables required to investigate the critical behavior of the system. In the simplex representation we have that:

$$H = -\sum_{\langle i,j \rangle} J'_{ij}\, \boldsymbol{S}_i \cdot \boldsymbol{S}_j\,. \tag{3}$$

The couplings in the simplex representation have the form

$$J'_{ij} = \frac{p-1}{p} J_{ij}\,. \tag{4}$$

The spin glass behavior is studied via a properly defined tensorial overlap between two *replicas* (independent copies of the system characterized by the same quenched disorder variables J_{ij}). Its Fourier transform (with wave vector $\boldsymbol{k}$) is given by[5]

$$q^{\mu\nu}(\boldsymbol{k}) = \frac{1}{V}\sum_i S_i^{(1)\mu} S_i^{(2)\nu} \mathrm{e}^{i\boldsymbol{k}\cdot\boldsymbol{R}_i}\,, \tag{5}$$

where $S_i^{(1)\mu}$ is the μ component of the spin at site i of the first replica in the simplex representation, $S_i^{(2)\nu}$ the ν component of the spin at site i in the second replica, and $V = L^3$ is the volume of the system.

This spin glass order parameter is then used to define the spin glass susceptibility in Fourier space.

$$\chi_q(\boldsymbol{k}) \equiv V \sum_{\mu,\nu} \overline{\langle |q^{\mu\nu}(\boldsymbol{k})|^2 \rangle}\,, \tag{6}$$

where $\langle(\cdots)\rangle$ indicates a thermal average and $\overline{(\cdots)}$ denotes the average over different realizations of the disorder (*samples* in the following). With the above definition, $\chi_q(0)$ is the usual spin glass susceptibility.

We are interested in studying the value of the dimensionless correlation length ξ/L, since at the transition temperature it does not depend on L, and is therefore extremely helpful to estimate the critical temperature value T_c: in fact one can usually simulate different lattice sizes, and look for the crossing point in the plot of the different ξ/L values. One can derive[6] the value of the correlation length ξ from the Fourier transforms of the susceptibility with

$$\xi = \frac{1}{2\sin(\boldsymbol{k}_{\mathrm{m}}/2)} \left(\frac{\chi_q(0)}{\chi_q(\boldsymbol{k}_{\mathrm{m}})} - 1 \right)^{1/2}\,, \tag{7}$$

where $\boldsymbol{k}_{\mathrm{m}}$ is the minimum wave vector allowed in the lattice. With the periodic boundary conditions used in this work we have $\boldsymbol{k}_{\mathrm{m}} = (2\pi/L, 0, 0)$ or any of the two vectors obtained permuting the indexes.

We also study the ferromagnetic properties of the model by monitoring the usual magnetization

$$\boldsymbol{m} = \frac{1}{V}\sum_i \boldsymbol{S}_i\,, \tag{8}$$

and correspondingly the magnetic susceptibility

$$\chi_m \equiv V\,\overline{\langle |\boldsymbol{m}|^2 \rangle}\,. \tag{9}$$

These two observables are crucial to check the possible existence of a ferromagnetic phase, as predicted by the mean field approximation of this model[7].

III. NUMERICAL METHODS

We have analyzed the DPM with 5 and with 6 states, on a number of lattice sizes ($L = 4$, 6, 8, and 12). All the numerical simulations have been run using a standard Metropolis algorithm combined with the Parallel Tempering (PT) optimized algorithm, in order to improve performances and allow to reach thermalization despite the very large relaxation times typical of spin glass models.

We define a Monte Carlo sweep (MCS) as a set of V trial updates of lattice spins. Each simulation consists on a thermalization phase, during which the system is brought to equilibrium, and a phase of equilibrium dynamics in which relevant physical observables are measured. As we require high quality random numbers, we use a 32-bit Parisi-Rapuano shift register[8] pseudo-random number generator.[20]

In order to improve the simulation performance and to speed up thermalization we apply a step of the PT algorithm[9] every few MCS's of the Metropolis algorithm. The PT algorithm is based on the parallel simulation of various copies of the system, that are governed by different values of temperature, and on the exchange of their temperatures according to the algorithm's rules. In practice we let the different configurations evolve independently for a few MCS, and then we attempt a temperature swap between all pairs of neighboring temperatures: the aim is to let each configuration wander in the allowed temperature range (that goes from low T values, smaller than T_c, to high T values, larger than T_c), and to use the decorrelation due to the high T part of the landscape to achieve a substantial speed up.

In order to check the time scales of the dynamical process, so as to assess the thermalization and the statistical significance of our statistical samples, we have computed a number of dynamical observables that characterize the PT dynamics.

One of them is the temperature-temperature time correlation function, introduced in Ref. 10, that we briefly recall. Let $\beta^{(i)}(t)$ be the inverse temperature of the system i at time t ($i = 0, \ldots, N_T - 1$), where N_T is

the total number of systems evolving in parallel in the PT.[21] We consider an arbitrary function of the system temperature, $f(\beta)$, changing sign at β_c. We shall name $f_t^{(i)} = f(\beta^{(i)}(t))$. In equilibrium, system i can be found at any of the N_T with uniform probability, hence $\langle f_t^{(i)} \rangle = \sum_{k=0}^{N_T-1} f(\beta_k)/N_T$, for all i and all t. We must choose a function f as simple as possible, such that $\sum_{k=0}^{N_T-1} f(\beta_k) = 0$.[22] Next, we can define the correlation functions

$$C_f^{(i)}(t) = \frac{1}{N-|t|} \sum_{s=1}^{N-|t|} f_s^{(i)} f_{s+|t|}^{(i)} \,, \tag{10}$$

$$\rho_f^{(i)}(t) = \frac{C_f^{(i)}(t)}{C_f^{(i)}(0)} \,, \tag{11}$$

where N is the total simulation time. To gain statistics we consider the sum over all the systems

$$\rho_f(t) = \frac{1}{N_T} \sum_{i=0}^{N_T-1} \rho_f^{(i)}(t) \,. \tag{12}$$

Notice that this correlation function measures correlations for a given copy of the system, that is characterized, during the dynamics, by different temperature values.

We have characterized the correlation function $\rho_f(t)$ through its integrated autocorrelation time[6,11]:

$$\tau_{\rm int} = \int_0^{\Lambda_{\rm int}} dt \; \rho_f(t) \,, \tag{13}$$

where $\Lambda_{\rm int} = \omega \, \tau_{\rm int}$ and we have used $\omega = 10$ (we have always used a total simulation time larger than 15 or 20 times $\tau_{\rm int}$).

We have studied the systems defined on the smaller lattices ($L = 4$ and 6) on standard PCs, while for the larger lattice sizes we have used the Janus computer[2,3], an FPGA-based machine specifically designed to handle simulations of spin glass models. The performance improvement offered by Janus allowed us to thermalize lattices of size up to $L = 12$. While the thermalization of lattices with $L = 8$ was relatively fast, the bigger lattice sizes proved to be rather difficult to equilibrate, even within Janus, things getting worse as the number of Potts states increases.

Tables I and II summarize the details about the numerical simulations respectively for the $p = 5$ and the $p = 6$ case. We were able to thermalize a large number of samples for L up to 12. The thermalization of $L = 16$ is possible, but it requires a dramatically large investment in computer resources, since the time required by each sample is very large. Because of that, and given the resources we could count upon, we have only been able to analyze a few samples: the results for the few samples that we have studied in this case are consistent with the ones obtained from the smaller sizes. In addition,

L	$N_{\rm samples}$	$\rm MCS_{min}$	$[\beta_{\rm min}, \beta_{\rm max}]$	N_β	$N_{\rm Metropolis}$	N_m
4	2400	10^7	[1.6, 9.5]	18	5	10^3
6	2400	2×10^7	[1.6, 9.5]	22	5	10^3
8	2448	4×10^8	[1.7, 6.5]	24	10	2×10^5
12	2451	6×10^9	[1.8, 5.5]	20	10	2×10^5

TABLE I: Details of the simulations for $p = 5$. $N_{\rm samples}$ is the number of samples (i.e. of the disorder realizations that we have analyzed), $\rm MCS_{min}$ is the minimum number of MCSs that we have performed, $[\beta_{\rm min}, \beta_{\rm max}]$ is the range of inverse temperatures simulated in the PT, N_β is the number of temperatures inside this interval, $N_{\rm Metropolis}$ is the frequency of the Metropolis sweeps per PT step, and $N_{\rm m}$ is the total number of measurements performed within each sample.

L	$N_{\rm samples}$	$\rm MCS_{min}$	$[\beta_{\rm min}, \beta_{\rm max}]$	N_β	$N_{\rm Metropolis}$	N_m
4	2400	10^7	[2.1, 9.8]	10	5	10^3
6	2400	2×10^7	[2.0, 9.65]	16	5	10^3
8	1280	10^9	[1.7, 7.5]	30	10	2×10^5
12	1196	6×10^{10}	[1.6, 6.5]	22	10	2×10^5

TABLE II: As in table I, but for $p = 6$.

for some samples with $L = 8$ and $L = 12$, which were especially difficult to thermalize, we had to use larger numbers of MCS's: see section IV A.

The number of Metropolis sweeps per PT step is 10 on Janus and 5 on the PC, and there is an important reason for that: in a standard computer the time needed for a step of the PT algorithm is small compared with a complete Metropolis MCS. This is not true on Janus, where it takes longer to perform a PT step than an Metropolis MCS: because of that, after a careful test of the overall simulation performance, we decided to lower the PT to Metropolis MCS ratio in order to increase Janus efficiency.

In the $p = 5$ case a numerical simulation of a single sample (thermalization plus measurements) on Janus takes 39 minutes for $L = 8$ and 10 hours on $L = 12$. The same simulations would require 7.4 days of an Intel$^{(R)}$ Core2Duo$^{(TM)}$ 2.4 GHz processor for $L = 8$ and 315 days for $L = 12$. These values grow when $p = 6$: here the equilibration takes 120 minutes for an $L = 8$ sample and 110 hours for $L = 12$ (on the PC they would take 24 days for $L = 8$ and 10 years for $L = 12$).

The results shown in this paper for the $p = 5$ model would have required approximately 2150 equivalent years of an Intel$^{(R)}$ Core2Duo$^{(TM)}$ 2.4 GHz processor: the ones for $p = 6$ would have required 12000 years.

IV. RESULTS

A. Thermalization Tests

Thermalization tests are a crucial component of spin glass simulations. Before starting to collect relevant results from the data we have to be sure that they are actually taken from a properly thermalized system, and are not biased from spurious effects.

A standard analysis scheme consists in evaluating the average value of an observable on geometrically increasing time intervals. The whole set of measurements is divided in subsets, each of which covers only part of the system's history (the last *bin* covers the last half of the measurements, the previous bin takes the preceding quarter, the previous bin the previous eighth and so on), and observables are averaged within each bin. The convergence to equilibrium is checked comparing the results over different bins: stability in the last three bins within error bars (that need to be estimated in an accurate way) is a good indicator of thermalization.

We show in figures 1 and 2 the logarithmic binning of ξ, as defined in equation (7), in the $p = 5$ and $p = 6$ cases. The compatible (and stable) values for the three last points satisfy the thermalization test explained above. The data in the plots are for the lowest temperature used on each lattice size: this is expected to be the slowest mode of the system, and its thermalization guarantees that also data at higher temperature values are thermalized. The plateau in the last part of each plot is a clear signal of proper thermalization: only data from the last bin are eventually used to compute thermal averages.

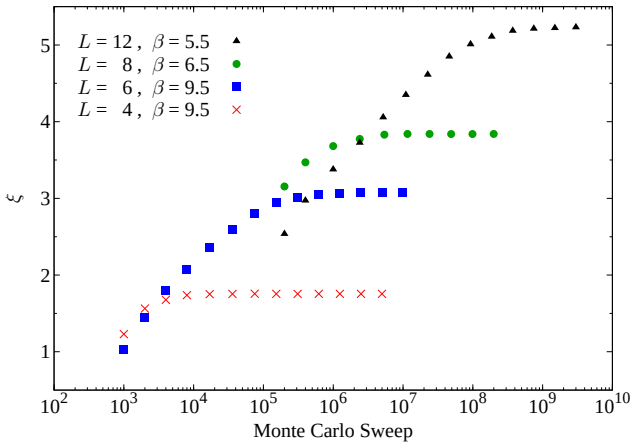

FIG. 1: Log-binning thermalization test for $p = 5$. For all data points the point size is bigger than the corresponding error bar.

We have also investigated how thermalization is reached in the individual samples (as opposed to the information on averages obtained from figures 1 and 2): to do that we have studied the correlation function for the temperature random walk defined in (12) and its associated integrated autocorrelation time, $\tau_{\rm int}$, defined in (13). As an example we plot in figure 3 the autocorrelation function (12) for a given sample as a function of the Monte Carlo time (here $L = 8$ and $p = 6$): one can see a fast, exponential decay in the left part of the figure, and (large) fluctuations around zero at later times.

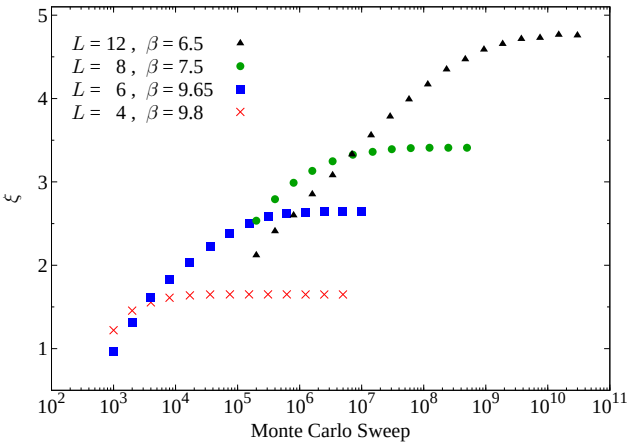

FIG. 2: As in figure 1, but $p = 6$.

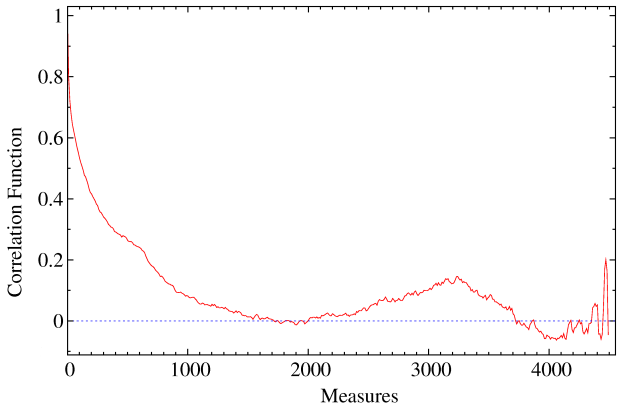

FIG. 3: The autocorrelation function (12) for one generic sample ($p = 6$, $L = 8$).

Sample to sample fluctuations of $\tau_{\rm int}$ are very large: in figure 4 we plot $\tau_{\rm int}$ for all our samples with $p = 5$, $L = 8$. In order to be on the safe side we have increased the number of MCS, by continuing the numerical simulation for a further extent, in all samples where our estimate of $\tau_{\rm int}$ was bigger than the length of the simulation divided by a constant c ($c = 20$ for $L = 8$ and $c = 15$ for $L = 12$, where achieving thermalization is much more difficult).[23]

B. Critical temperature and critical exponents

Our analysis of the critical exponents of the system has been based on the quotient method[6,12]: by using the averaged value of a given observable O measured in lat-

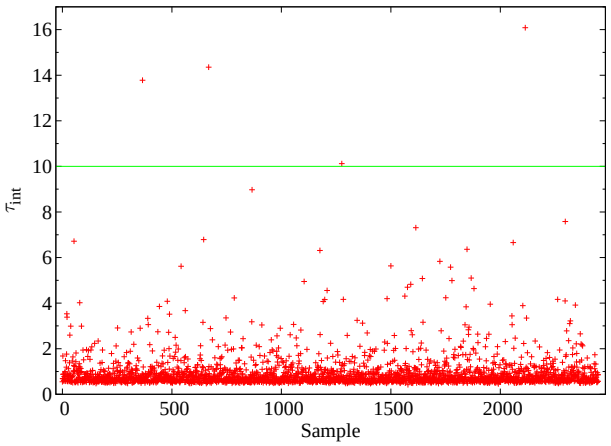

FIG. 4: Integrated autocorrelation time, $\tau_{\rm int}$, for all $p = 5$, $L = 8$ samples. $\tau_{\rm int}$ is in units of blocks of ten measurements, i.e. of 2010^3 MCS. Samples above the green line have been "extended" (see the text for a discussion of this issue).

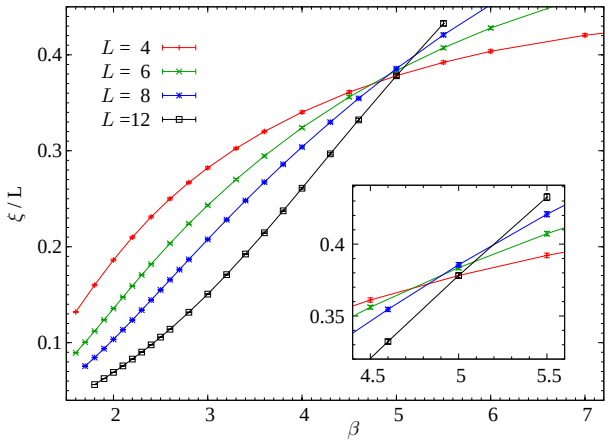

FIG. 5: Overlap correlation length in lattice size units as a function of the inverse temperature β for $L = 4$, 6, 8 and 12. Here $p = 5$.

tices of different sizes, we can estimate its leading critical exponent x_O,

$$\overline{\langle O(\beta)\rangle} \approx |\beta - \beta_c|^{-x_O} \,. \tag{14}$$

By considering two systems on lattices of linear sizes L and sL respectively one has that[6,12]

$$\frac{\overline{\langle O(\beta, sL)\rangle}}{\overline{\langle O(\beta, L)\rangle}} = s^{x_O/\nu} + O(L^{-\omega}) \,, \tag{15}$$

where ν is the critical exponent of the correlation length and ω is the exponent of the leading-order scaling-corrections[6].

We use the operators $\partial_\beta \xi$, from (7), and χ_q, from (6) in equation (15) to obtain respectively the critical exponents $1 + 1/\nu$ and $2 - \eta_q$. The exponent $2 - \eta_m$ is obtained applying eq. (15) to the magnetic susceptibility χ_m, from (9).

To use the quotient method we start estimating the finite-size transition temperature: we do this by looking at the crossing points of the correlation length in lattice units (ξ/L) for various lattice sizes. We have used a cubic spline interpolating procedure to compute both the crossings of ξ/L and its β-derivative (we have followed the approach described in detail in Ref. 13).

We show in figures 5 and 6 the behavior of ξ/L as a function of β. The different curves are for different lattice sizes. The crossing points are rather clear in both cases, giving a strong hint of the occurrence of a second order phase transition. At least for $p = 5$ scaling corrections play a visible role, and the crossing points undergo a small but clear drift towards lower temperatures for increasing lattice sizes. We summarize in tables III and IV the β values of the crossing points for two different pairs of lattice sizes, together with the estimated values of the critical exponents ν and η_q that we obtain using relation (15).

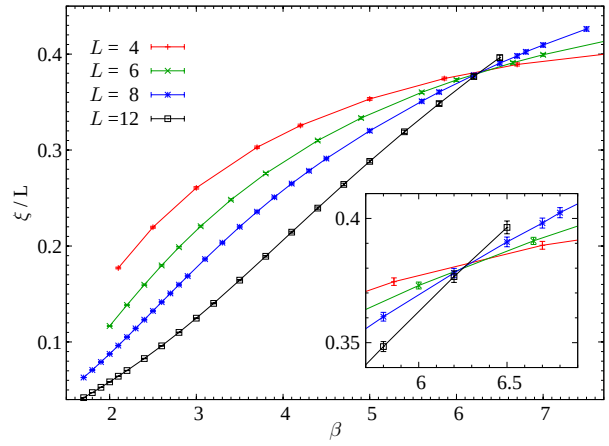

FIG. 6: As in figure 5, but $p = 6$.

Since we can only get reliable results on small and medium size lattice we cannot control in full scaling corrections, and a systematic extrapolation to the infinite volume limit is impossible. It is clear however that the effective critical exponents summarized in tables III and IV do not suggest that asymptotically for large volume the system will not be critical (in this case, for example, η_q should be asymptotically equal to 2): our numerical data clearly support the existence of a finite temperature phase transition.

(L_1, L_2)	$\beta_{\rm cross}(L_1, L_2)$	$\nu(L_1, L_2)$	$\eta_q(L_1, L_2)$	$\eta_m(L_1, L_2)$
$(4, 8)$	4.83(5)	0.82(3)	0.13(2)	1.72(2)
$(6, 12)$	5.01(4)	0.81(2)	0.16(2)	1.94(2)

TABLE III: Numerical values of our estimates for the crossing point of the curves ξ/L. We give $\beta_{\rm cross}$, the thermal critical exponent ν, the anomalous dimension of the overlap η_q, and the anomalous dimension of the magnetization η_m.

(L_1, L_2)	$\beta_{\rm cross}(L_1, L_2)$	$\nu(L_1, L_2)$	$\eta_q(L_1, L_2)$	$\eta_m(L_1, L_2)$
$(4, 8)$	6.30(9)	0.80(2)	0.10(2)	1.453(19)
$(6, 12)$	6.26(7)	0.80(4)	0.16(2)	1.971(19)

TABLE IV: As in table III, but $p = 6$.

We take as our best estimates for the critical exponents the one obtained from the lattices with sizes $L = 6$ and $L = 12$. For $p = 5$

$$\beta_c = 5.01(4)\,,\ \nu = 0.81(2)\,,\ \eta_q = 0.16(2)\,, \qquad (16)$$

while for $p = 6$.

$$\beta_c = 6.26(7)\,,\ \nu = 0.80(4)\,,\ \eta_q = 0.16(2)\,. \qquad (17)$$

It is interesting to compare these values with those of other Potts models with a different number of states. In particular we are interested in the value of the critical exponents as a function of the number of states, since we want to characterize the critical behavior of the various models and attempt a prediction of the model's behavior when the number of states is large. In our particular model and with the (low) values of the temperature that are interesting for us (since we need to get below the critical point) even with the large computational power available to us thanks to Janus the simulation for $p = 8$, say, on a $L = 12$ lattice, would require an unavailable amount of CPU time. What is found in the very interesting work of Refs. 1 and 5 is different, since there one is able to thermalize a $p = 10$ model on a large lattice, and no transition is observed. The model analyzed in these two references[1,5] is indeed slightly (or maybe, it will turn out, not so slightly) different from the present one, since there $\overline{J}$ is negative. It is not clear to us if this difference could explain a quite dramatic discrepancy of the observed behavior, or if, for example, a different (very low) temperature regime should be analyzed to observe relevant phenomena: this is surely an interesting question to clarify, and the fact that the coupling have a negative expectation value, reducing in this way frustration, could turn out to make a difference.

C. Absence of ferromagnetic ordering in the critical region

Our DPM is in principle allowed to undergo a ferromagnetic phase transition (since no symmetry protects it), and at low temperatures could present a spontaneous magnetization, as discussed in Ref. [13]. Because of that we have carefully studied the magnetic behavior of the model at low temperatures. We have analyzed both the magnetization and the magnetic susceptibility below the spin glass critical point.

In the paramagnetic phase the magnetization is random in sign, and its absolute value is expected to be proportional to $1/\sqrt{V}$. In Figs. 7 and 8 we check whether

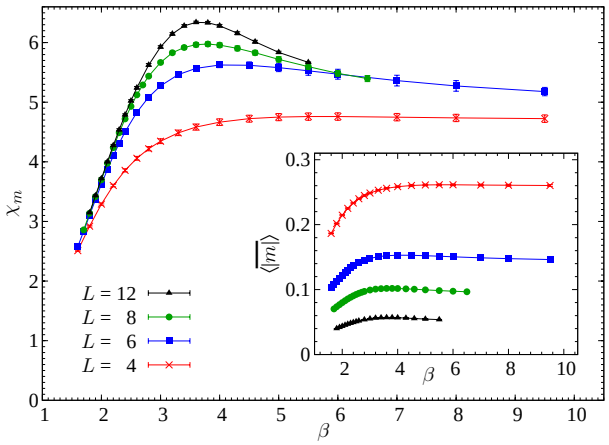

FIG. 7: Magnetic susceptibility as a function of β for $L = 4$, 6, 8 and 12. Here $p = 5$.

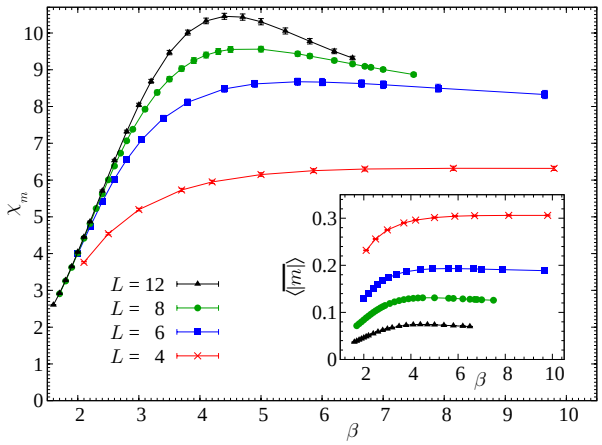

FIG. 8: As in figure 7, but $p = 6$.

$\overline{\langle |\boldsymbol{m}| \rangle}$ around the spin glass critical region tends to an asymptotic value for larger lattice size, or not. From the figures we see $\overline{\langle |\boldsymbol{m}| \rangle}$ goes to zero in the critical region. Also, we studied the magnetic susceptibility $\chi_m = V\overline{\langle |\boldsymbol{m}|^2 \rangle}$ which is independent of size. Again in Figs. 7 and 8 we check that, and we see a non-divergent behavior. This behavior is extremely different from a ferromagnetic phase in which χ_m diverges as the volume.

Besides, as reported in Sec. IV B the exponent η_m is close to 2, so we could say that a ferromagnetic-paramagnetic phase transition does not happen in the range of temperatures that we have studied.

V. EVOLUTION OF CRITICAL EXPONENTS WITH p

In table V we summarize the values of the inverse critical temperature and of the thermal and overlap critical exponents for DPM from $p = 2$ (the Ising, Edwards-Anderson spin glass) up to $p = 6$. We also plot these

data items in figure 9.

From table V and figure 9 some results emerge very clearly. First, the inverse critical temperature roughly follows a linear behavior in p, with a slope very close to one. We have added in table V the ratio (R) between the numerical determinations (in $3d$) of $\beta_c(p)$ and their values in the Mean Field (MF) approximation. One can see that the large deviations from the MF prediction occur for large values of p (notice that $R > 1$ since MF suppresses fluctuations).[24]

Second, ν decreases monotonically and η_q grows monotonically with the number of states p. To discuss this behavior it is useful to keep in mind that when using finite size scaling to study a disordered first order phase transition one expects to find[14] $\nu = 2/D$ and $2 - \eta_q = D/2$, i.e., in our $D = 3$ case, $\nu = 2/3$ and $\eta_q = 1/2$. These are "effective" exponents, that are a bound to the ones allowed for second order phase transitions.

Both sets of values for ν and η_q are indeed completely compatible with tending, as p increases, to those limit values that characterize a first order phase transition. If this turns out, as our numerical data make very plausible to be true, two different scenarios open. The first possibility is that the p-states DPM undergoes a disordered first order phase transition for large enough values of p (just as in the ordered Potts model, that for $p \geq 3$ undergoes a first order phase transition), while the second possibility is that the DPM will show a standard second order phase transition for all finite values of p. This is the typical issue that is very difficult to settle with numerical work: an analytical solution of the model with infinite number of states would be very useful as a starting point in order to discriminate between these two possible scenarios.

p	β_c	ν	η_q	R
2 (Ref.[15])	1.786(6)	2.39(5) [a]	$-0.366(16)$ [b]	2.187(8)
2 (Ref.[16])	1.804(16)	2.45(15)	$-0.375(10)$	2.209(20)
3 (Ref.[5])	2.653(35)	0.91(2)	0.02(2)	2.17(3)
4 (Ref.[13])	4.000(48)	0.96(8)	0.12(6)	2.45(3)
5 (this paper)	5.010(40)	0.81(2)	0.16(2)	2.51(2)
6 (this paper)	6.262(71)	0.80(4)	0.16(2)	2.69(3)

[a] This value of ν is from ξ_L/L. It is different and more reliable than the one obtained from the spin glass susceptibility, that, because of large scaling corrections, would severely depend on the kind of analysis.

[b] This value of η_q is from the study of the spin glass susceptibility.

TABLE V: Critical parameters as a function of p. All data are for binary couplings, with zero expectation value. By R we denote the ratio between the critical β in three dimensions and that computed in Mean Field.

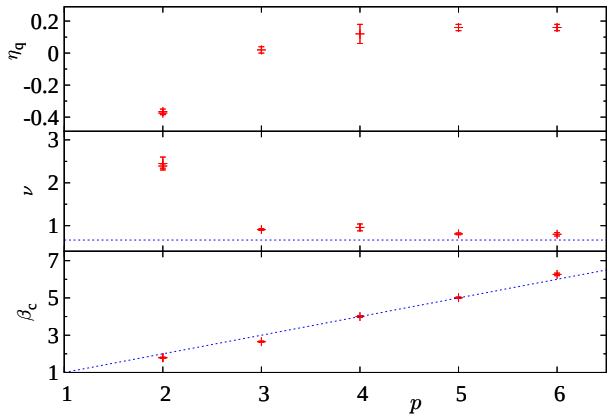

FIG. 9: In the bottom plot: β_c versus p, and the straight line $f(p) = p$. Middle plot: ν as a function of p. We also show (dashed line) the value which marks the onset of a disordered first order phase transition ($\nu_{\rm first} = 2/3$). Upper plot: η_q as a function of p.

VI. CONCLUSIONS

In this note we have characterized the critical behavior of the $3D$ DPM with $p = 5$ and $p = 6$, i.e. with a reasonably large number of states. Our numerical simulations have allowed us to reach some clear evidences, and to stress some difficult issues that will require further analysis.

We first stress that in both cases the spin glass transition is very clear, and we have been able to obtain a reliable estimate of the critical temperature and of the critical exponents ν and η_q. We have discussed what happens when p increases; we have found that β_c increases like p. A similar result was conjectured in Ref. 18 (for all values of p) analyzing high temperature series and found in Mean Field for $p \leq 4$ (although, of course, the slope is wrong). In addition, the behavior of ν and η_q is compatible with going to the large p limit value that characterizes a first order phase transition.

In the low temperature regime we do not see any sign of a transition to a ferromagnetic regime, that would be in principle allowed by the structure of our model. We cannot exclude that at very low T values something would happen, but in all the range we can explore the system stays in the spin glass phase.

A last piece of important evidence is that low temperature simulations of this model look difficult, and that they slow down severely for increasing p. In our particular model, where the expectation of the coupling is zero, it would be impossible to study reliably a $p = 8$ model with the computational resources available today.

This last observations opens indeed a last point that it will be interesting to analyze in the future. When couplings have a negative expectation value the simulation of a $p = 10$ model [1,5] is possibly easier than it would be in

our case, and the results are very different: in that case one does not see any sign of a phase transition. Analyzing how the DPM depends on the expectation value of the couplings is indeed at this point a crucial issue, since it could turn out that the reduction in frustration due to a negative net value of the couplings could completely change the critical behavior of the model.

Acknowledgments

Janus has been funded by European Union (FEDER) funds, Diputación General de Aragón (Spain), by a Microsoft Award - Sapienza - Italy, and by Eurotech. We were partially supported by MICINN (Spain), through contracts No. TEC2007-64188, FIS2006-08533-C03, FIS2007-60977, FIS2009-12648-C03 and UCM-Banco de Santander. D. Yllanes and B. Seoane are FPU Fellow (Spain). S.P.-G. was supported by FECYT (Spain). The authors would like to thank the Arénaire team, especially J. Detrey and F. de Dinechin for the VHDL code of the logarithm function[19].

[1] C. Brangian, W. Kob and K. Binder, Europhys. Lett. **53**, 756-761 (2001), preprint arXiv:cond-mat/0009475; Phil. Mag. B **82**, 663 (2002), preprint arXiv:cond-mat/0104355; J. Phys. A : Math. Gen. **35**, 191 (2002), preprint arXiv:cond-mat/0106314; Europhys. Lett. **59**, 546 (2002), preprint arXiv:cond-mat/0202232; J. Phys. A: Math. Gen. **36**, (2003) 10847, preprint arXiv:cond-mat/0211195.

[2] F. Belletti, M. Cotallo, A. Cruz, L. A. Fernández, A. Gordillo, A. Maiorano, F. Mantovani, E. Marinari, V. Martin-Mayor, A. Muñoz-Sudupe, D. Navarro, S. Perez-Gaviro, J. J. Ruiz-Lorenzo, S. F. Schifano, D. Sciretti, A. Tarancón, R. Tripiccione and J. L. Velasco, Comp. Phys. Comm. **178**, 208 (2008).

[3] F. Belletti, M. Cotallo, A. Cruz, L. A. Fernández, A. Gordillo-Guerrero, A. Maiorano, F. Mantovani, E. Marinari, V. Martin-Mayor, A. Muñoz-Sudupe, D. Navarro, S. Perez-Gaviro, M. Rossi, J. J. Ruiz-Lorenzo, S. F. Schifano, D. Sciretti, A. Tarancón, R. Tripiccione, J. L. Velasco, G. Zanier and D. Yllanes, Computing in Science & Engineering **11**, 48 (2009).

[4] H. Nishimori and M. J. Stefen, Phys. Rev. B, **27**, 5644 (1983). E. Marinari, S. Mossa and G. Parisi, Phys. Rev. B **59** 8401 (1999); L. A. Fernández, A. Maiorano, V. Martin-Mayor, D. Navarro, D. Sciretti, A. Tarancón and J. L. Velasco, Phys. Rev. B **77**, 104432 (2008). D. M. Carlucci, Phys. Rev. B **60**, 9862 (1999). J.L. Jacobsen and M. Picco, Phys. Rev B **65**, 026113 (2002).

[5] L. W. Lee, H. G. Katzgraber and A. P. Young, Phys Rev. B **74**, 104416 (2006).

[6] See for example D. J. Amit and V. Martin-Mayor, *Field Theory, the Renormalization Group and Critical Phenomena,* (World-Scientific, Singapore, third edition, 2005).

[7] D. Elderfield and D. Sherrington, J. Phys.C **16**, L497 (1983). D. Elderfield and D. Sherrington, J. Phys.C **16**, L971 (1983). D. J. Gross, I. Kanter and H. Sompolinsky, Phys. Rev. Lett. **55**, 304 (1985).

[8] G. Parisi and F. Rapuano, Phys. Lett. B **157**, 301 (1985).

[9] M. Tesi, E. Janse van Resburg, E. Orlandini and S. G. Whillington, J. Stat. Phys. **82**, 155 (1996); K. Hukushima and K. Nemoto, J. Phys. Soc. Jpn. **65**, 1604 (1996); E. Marinari, *Optimized Monte Carlo Methods*, in *Advances in Computer Simulation*, edited by J. Kertész and Imre Kondor (Springer-Verlag, Berlin 1998), preprint arXiv:cond-mat/9612010; E. Marinari, G. Parisi and J. J. Ruiz-Lorenzo, *Numerical Simulations of Spin Glass Systems* in *Spin Glasses and Random Fields*, edited by A. P. Young (World Scientific, Singapore, 1997).

[10] L.A. Fernandez, V. Martin-Mayor, S. Perez-Gaviro, A. Tarancon and A.P. Young Phys. Rev. B 80, 024422 (2009).

[11] A. D. Sokal, *Functional Integration. Basis and Applications*, lectures given at the 1996 Cargèse Summer School, edited by C. DeWitt-Morette, P. Cartier and A. Folacci (Plenum, New York, USA 1997).

[12] H. G. Ballesteros, L. A. Fernández, V. Martín-Mayor and A. Muñoz Sudupe, Phys. Lett. B **378**, 207 (1996).

[13] A. Cruz, L. A. Fernández, A. Gordillo-Guerrero, M. Guidetti, A. Maiorano, F. Mantovani, E. Marinari, V. Martín-Mayor, A. Muñoz Sudupe, D. Navarro, G. Parisi, S. Pérez Gaviro, J. J. Ruiz Lorenzo, S. F. Schifano, D. Sciretti, A. Tarancón, R. Tripiccione, J. L. Velasco, D. Yllanes and A. P. Young, Phys. Rev. B **79**, 184408 (2009).

[14] A. Maiorano, V. Martin-Mayor, J. J. Ruiz-Lorenzo and A. Tarancon, Phys. Rev. B **76**, 064435 (2007).

[15] H. G. Katzgraber, M. Körner and A. P. Young , Phys. Rev. B **73**, 224432 (2006)

[16] M. Hasenbusch, A. Pelissetto and E. Vicari, Phys. Rev. B **78**, (2008) 214205.

[17] T. R. Kirkpatrick and P. G. Wolynes. Phys. Rev. B **36**, 8552 (1987).

[18] B. Lobe, W. Janke and K. Binder. Eur. Phys. J. B **7**, 283 (1999).

[19] J. Detrey and F. de Dinechin, Microprocessors and Microsystems **31**, 537 (2007).

[20] Our FPGA did not have components to accomodate the L=12 code with a 48 bits generator (that could instead be used for L=8). We have performed additional numerical simulations in the smaller lattices, on PC, using 64 bits random numbers and in the $L = 8$, on Janus, using 48 bits random numbers. We have reproduced in all cases, within statistical errors, the results obtained with the 32 bits generator.

[21] We have used β's not uniformly distributed in order to have a PT acceptance of order 30-40% in the whole β-interval. In addition, we have include additional β's in the critical region to have clearer crossing points of the correlation length.

[22] Our choice of $f(\cdot)$ is slightly different from that of Ref. 10; $f(\beta) = a(\beta - \beta_c)$ for $\beta < \beta_c$, and $f(\beta) = b(\beta - \beta_c)$ for $\beta > \beta_c$. The ratio of the slopes a/b is fixed by the con-

dition $\sum_{k=0}^{N_T-1} f(\beta_k) = 0$. The overall normalization being irrelevant, we choose $a = 1$.

[23] In the $p = 5$, $L = 8$ case for 2442 samples we have run a simulation of total extent $\eta = 4 \times 10^8$ MCSs, while for 5 samples $\eta = 8 \times 10^8$ MCSs, and for 1 sample $\eta = 1.6 \times 10^9$ MCS. In the $p = 5$, $L = 12$ case for 2382 samples $\eta = 6 \times 10^9$ MCSs, for 54 samples $\eta = 1.2 \times 10^{10}$, for 8 samples $\eta = 2.4 \times 10^{10}$, and for 7 samples $\eta = 4.8 \times 10^{10}$ MCS. In the $p = 6$, $L = 8$ case: for 1263 samples $\eta = 10^9$ MCSs, for 8 samples $\eta = 2 \times 10^9$ and for 9 samples $\eta = 4 \times 10^9$. In the $p = 6$, $L = 12$ case for 1173 samples $\eta = 6 \times 10^{10}$ MCSs, for 17 samples $\eta = 1.2 \times 10^{11}$ MCSs and for 6 samples $\eta = 2.4 \times 10^{11}$ MCSs.

[24] In the MF approximation was obtained, using the Hamiltonian[7,17],

$$\mathcal{H} \equiv -\frac{p}{2} \sum_{i \neq j} J_{ij}\, \delta_{s_i, s_j}\,,$$

that $T_c/J = 1$ for $p \leq 4$ and $(T_c/J)^2 = 1 + (p-4)^2/42 + O((p-4)^4)$ for $p > 4$. In addition for very large p, $T_c/J \simeq \frac{1}{2}\,(p/\log p)^{1/2}$. Taking into account the extra p factor in the Hamiltonian used in the Mean Field and the fact that $J = \sqrt{2d}\ (\overline{J_{ij}^2} = J^2/N$, being N the number of spins in the MF computation) since we are working in finite dimension (d), we obtain the finite dimension version of the critical β using the Mean Field approximation: $\beta_c = p/\sqrt{2d}$ for $p \leq 4$ and $\beta_c = \frac{p}{\sqrt{2d}}\left(1 - (p-4)^2/84 + O((p-4)^4)\right)$ for $p > 4$ (notice the minus signum of the $(p-4)^2$ correction); in addition, for large p, one obtains $\beta_c \simeq \sqrt{\frac{2}{d}}\,(p \log p)^{1/2}$. Note that in our case $\sqrt{2d} \simeq 2.45$.